

Ultrasonic defect detection in wooden pallet parts for quality sorting

Daniel L. Schmoldt

USDA Forest Service, Southern Research Station
Brooks Forest Products Center, Blacksburg VA 24061-0503

Robert M. Nelson

USDA Forest Service, Southern Research Station
One Gifford Pinchot Drive, Madison WI 53705

Robert J. Ross

USDA Forest Service, Forest Products Laboratory
One Gifford Pinchot Drive, Madison WI 53705

ABSTRACT

Millions of wooden pallets are discarded annually due to damage or because their low cost makes them readily disposable. Higher quality wooden pallets, however, can be built from high quality deckboards and stringers, and have a much longer life cycle and a lower cost per trip. The long-term goal of this project is to develop an automated pallet part inspection system to sort pallet parts according to grade. Ultrasonic time of flight (TOF) measurements in a pitch-catch arrangement are being used to distinguish different types of defects, including knots, decay, cross grain, and voids, from clear wood. Rolling transducers of 3 different frequencies (84 KHz, 0.5 MHz, and 1.25 MHz) have been used to collect measurements on four oak deckboards of 1/2" thickness. Ultrasonic C-scans taken on a 1/2" x 1/2" grid indicate that TOF with 84 KHz transducers can be used to partially distinguish between several deckboard features and clear wood. Nevertheless, future application of these results to defect detection must not be limited to single, pixel value classification, but must include pixel neighborhoods with textural information.

Keywords: ultrasound, wooden pallets, inspection, grading, defect detection, time of flight.

1. INTRODUCTION

Pallets are a critical component of our transportation infrastructure and a substantial sink for wood resources. Wooden pallets physically support a variety of raw and finished goods during freight transportation. In fact, one would be hard-pressed to find a product that did not spend part of its transportation life on a pallet, as either components or as finished product. While pallets are important for transportation, they also are significant from a wood resource use standpoint. Approximately 40% of all hardwood timber volume cut each year goes into the manufacture of pallets. Constructing longer lasting pallets serves the needs of the transportation industry and the desire to conserve valuable natural resources.

Most wooden pallets are constructed from two types of pallet parts (Figure 1): (1) stringers—the structural center members that support the pallet load and (2) deckboards—the top and bottom facing members that provide dimensional stability and product placement. There are many variants of this basic design, but most pallets contain solid wood components that are produced from lumber or from the center cant material of logs. Cant material has a high percentage of defect volume and is generally not highly valuable for other solid wood products. Non-cant lumber used in constructing pallets is low quality, also, and is undesirable for other wood products. Therefore, the pallet manufacturing industry must make use of low-quality raw materials and yet produce a product that remains in service for many trips.

Unfortunately, millions of wooden pallets are built annually with little concern for strength and durability. Often, individual pallets are constructed from a variety of wood species and from parts with different strength properties. Building pallets in this way results in pallets with random and unknown strength and durability. On the other hand, high quality wooden pallets can be manufactured from high quality pallet parts, which gives them a much longer life cycle and promotes their re-use. Nevertheless, unknown profit margins and untrained employees make manual grading and sorting of pallet

infeasible. Therefore, we have as a long-term goal to develop an automated pallet part inspection system. A previous study² indicated that the increased value of higher-quality pallets can justify expenditures in an automated grading and sorting system. We envision that such a system will scan moving parts in a production environment, locate and identify pallet part degrades, and grade the parts according to established visual grading rules. This study addresses the first 2 aspects of this research effort.

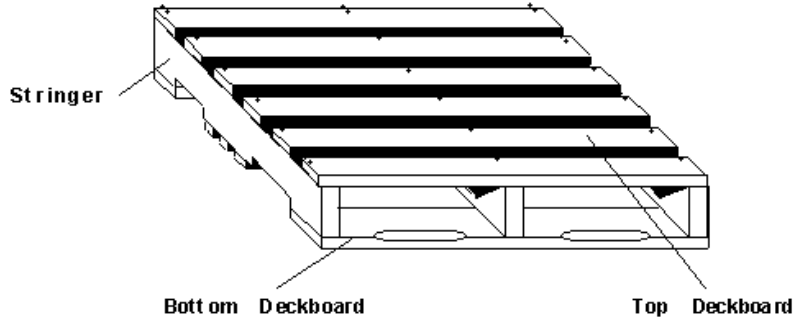


Figure 1. A typical stringer class wooden pallet contains three load-supporting stringers in the center and five to seven deckboards on both the top and bottom.

2.1 ULTRASOUND AND WOOD

2.1 Previous work

Earlier work has established that through transmission and reflection of ultrasonic signals convey much information about the internal structure of wood. In particular, ultrasound can: (1) detect knots in hardwood and softwood lumber⁵, (2) detect decay in structural timbers⁶, (3) evaluate the strength of structural members in situ⁷, (4) detect knots and decay in timber bridge members⁸⁻¹¹, (5) detect knots, decay, and cross grain in small laboratory samples³, (6) detect closed surface checks and honeycombs³ in dried red oak (*Quercus rubra* L.), and (7) be used to examine wooden art objects for small cracks and other degradation⁴. These studies used a variety of waveform parameters to detect defects, including: time of flight (or speed), peak amplitude, time to peak amplitude, centroid time, root mean square of the time domain signal, number of threshold crossings in the time domain, frequency domain modes, centroidal frequency, and frequency domain energy.

In most of these studies, however, either carefully prepared laboratory samples or surfaced lumber were examined. In the real world environment, however, pallet parts are low quality and rough sawn, and exhibit shifting axial geometry (so that geometry differs depending where on a surface one takes measurements). Preliminary work on pallet part scanning^{15,16} indicates that time of flight and peak amplitude may be insufficient for reliable defect detection. Work^{8,9,17} also supports this observation. Nevertheless, the preliminary nature of this investigation suggested the use of simpler TOF measurements to evaluate (1) rolling transducer signal transmission and (2) defect discrimination by different ultrasound frequencies.

While detecting the presence or absence of a defect may not be a difficult problem, specifying the location and extent of a defect within a pallet part are more difficult questions. From the manner in which pallet part defects are measured and evaluated (Table 1), i.e. by size, extent, and location, it is clear that ultrasound measurements taken at many points along the length of a part cannot provide sufficient information to properly grade the part. Rather, a 2-dimensional ultrasound image of the surface of the part will need to be constructed in order to locate, size, and identify grading defects.

2.2 Time of flight

Time of flight (TOF) is strongly affected by the grain orientation of the wood relative to the transducer. TOF is shortest when compression wave direction of travel is parallel to the grain, as is the case for knots and from end to end in a board³. TOF increases with: longer transmission distance, decay, higher moisture content, increasing grain angle away from parallel to the direction of transmission, lower density, transmission through air (as at checks, holes, and splits), and

poor coupling of transducer to the wood. TOF changes with orientation of the transducer relative to the growth rings—shortest TOF occurs when transmitting longitudinally. Greater TOF results for transmission perpendicular to the grain and also in the purely radial direction. Greater TOF occurs when transmitting in a purely tangential direction, and greatest TOF occurs when transmitting perpendicular to the grain and between purely tangential and purely radial directions³ Wood anisotropy complicates the interpretation of ultrasound signal transmission.

Table 1. Partial list of grading criteria employed for deckboards

Defect	Description	Grades		
		2 & BTR	3	4
Sound knots	Maximum dimension across width of the board	1/4 of board width	1/3 of board width	1/2 of board width
Location of knots	Knots in the edges and end 3" of the boards	1/2" diameter	1/4 of board width	1/3 of board width
Unsound knots/holes	Knot holes, unsound or loose knots, and holes	1/8 of board width	1/6 of board width	1/4 of board width
Cross grain	Slope of general cross grain	1" in 10"	1" in 8"	1" in 6"
	Max. dimension of local cross grain	1/4 board width	1/3 board width	1/2 board width
Splits, checks, and shake	Max. length singly or in combination	1/4 of board length	1/2 of board length	3/4 of board length
	Defects 3" or less are ignored			
Decay	Cross section deepest penetration	None allowed	1/8 of cross section	1/4 of cross section

In this study, we investigate the ability of time-of-flight (TOF) ultrasonics to detect pallet part degrades on deckboards. There are three primary issues that we address, including: (1) whether TOF can be used to distinguish between clear wood and between different types of flaws on pallet parts, (2) whether different frequency transducers vary in their ability to distinguish flaws, and (3) whether rolling transducers provide acceptable contact with the wood to generate repeatable measurements. Results obtained in this preliminary work will direct subsequent tests of ultrasonic detection and will enable us to build a laboratory prototype to continue data collection and for demonstration.

3. STUDY METHODS

3.1 Transducers and coupling

TOF was measured using transducers of three different center frequencies: 84 KHz, 0.5 MHz, and 1.25 MHz. An existing materials handling fixture was modified for use with the 0.5 MHz and 1.25 MHz transducers to allow sufficiently accurate positioning. Due to the difference in transducer size and design the larger 84 KHz transducers had to be used with a portable roll bed fixture³. Abbreviated specifications for the 3 transducers are given below.

(1) 84 KHz: James Instrument Inc.* Model C-7219 rolling transducers with a 84 KHz center frequency. The roller's diameter as measured is 3.194" on centerline, the width measures 1.322", and the surface material is lexan. The piezo-electric ceramic is type PZT-4 immersed in an oil filled cavity and enclosed in a stainless steel housing.

(2) 0.50 MHz: Staveley Sensors Inc., "Harrisonic" Model: RT-0005-16SY rolling transducers with a center frequency of 0.5 MHz. The low end frequency for this piezoelectric transducer is about 300 KHz. The roller is a nominal 25 mm diameter (1.0") having a nominal 10 mm wide (3/8") elastomer rubber pad.

(3) 1.25 MHz: Staveley Sensors Inc., "Harrisonic" Model RT-0105-16DY rolling transducers with a center frequency of 1.25 MHz. The low end of the spectrum for this piezoelectric transducer is about 600 KHz. As with the other Staveley transducers, the roller is a nominal 25 mm diameter (1.0") having a nominal 10 mm wide (3/8") elastomer rubber pad which gives a 10mm footprint.

Constant coupling was achieved by air pressure cylinders. A force was supplied to each of the transducers by a Bimba Co. air cylinder model 09-1.125-NR. The air to the piston was regulated to a constant 30 psig for the 0.5 MHz and 1.25 MHz transducers, and 40 psig for the 84 KHz transducer.

3.2 Experimental equipment

A James Instruments Inc. "V-meter" (Model C-4902) was used to send, receive, and display elapsed time of flight. The V-meter generates the voltage pulse to excite the piezo-electric transducer, senses the voltage pulse received from the receiving piezo-electric transducer, and provides the elapsed time between sending and receiving. Normally, the time for signal transmission on paths other than in the specimen and for signal processing must be subtracted out from the gross TOF reading to obtain an actual TOF value for the specimen. However, because our interest was in relative TOF values over a deckboard, this TOF correction was a constant bias that could be ignored.

The V-meter setting used in all tests was a pulse repetition frequency of 10. The transmitter voltage level selector switch was set to 500 Volts, and the measurement time base set to seconds. The V-meter generated a triggering pulse of 2 microseconds duration into the high voltage circuit. The duration of the pulse at the transducers, however, is somewhat dependent on the capacitance of the transducer itself.

Prior to measuring a test piece, the V-meter was calibrated using two James Instruments Inc. hand-held flat face non-rolling transducers, BNC type connectors, and a 25.6 microsecond aluminum standard bar of cylindrical cross section. Calibration consists of adjusting the set point potentiometer (dial) such that the liquid crystal display read 25.6 microseconds when the hand held transducers were in contact with the ends of the standard bar.

3.3 Deckboard samples

Four sample deckboards were obtained from a local pallet manufacturer. The boards are Northern red oak (*Quercus rubra*, L.) pallet deckboards 51" long, 3-3/8" wide, and 1/2" minimum thickness. Boards were designated QrD1 (*Quercus rubra* Deckboard 1), QrD2, QrD3, and QrD5. The samples contained various defects, such as knots, splits, and cross grain, in addition to clear wood.

Sample deckboards were obtained in fresh cut (green) condition. They were subsequently kept in a temperature and humidity controlled cabinet held at 36 degrees F, 82% relative humidity, for several months prior to testing. By the time of testing the boards had dried out to the same moisture content as the humidity cabinet. The result was that the effect of moisture content was blocked in these tests.

* Tradenames are used throughout this manuscript for informational purposes only. No endorsement by the U.S. Department of Agriculture or the U.S. Forest Service is implied.

3.4 Data collection

Because we were unable to automate the collection of C-scan data, taking measurements on entire deckboard samples was time prohibitive. Instead the most feature rich regions of the 4 deckboards were scanned. We set the spatial sampling rate to 1/2" in both the X and Y directions. Six scan lines were established on each sample, beginning with a scan line at 0.5" from a reference edge and ending with a line at 3.0" from the reference edge. The total length scanned on each board varied from 21" to 27" for the different deckboards. This produced a 1/2" x 1/2" grid on each sample deckboard. TOF values were measured on all four of these grids using each of the three transducers. In addition, repeated measurements were made with both the 0.5 MHz and 1.25 MHz transducers for two of the deckboards (QrD2 and QrD3). These two experiments were expected to provide answers to the questions posed in the study objectives noted above.

To effectively evaluate the feature discrimination capability of TOF values for the different transducers, we needed to objectively label the different regions, point by point, on each sample grid. Knots are easy to identify visually, but cross grain areas are not. In this study, wood fiber grain angle is the direction of the projection of the wood fibers onto the measurement surface. Grain angle measurements were made using a Metriguard model 510 grain angle indicator by positioning the boards by hand and recording the grain angle. Measurements of grain angle were made on both faces, with the average grain angle calculated as the arithmetic average of the two surface readings. The effect of grain angle in the board thickness plane was not considered in these tests.

Based on the grading criteria for pallet deckboards (Table 1), we used the cross grain categories mentioned there, i.e., 10-12.5% (greater than 1:10, but less than 1:8), 12.5-16.6% (greater than 1:8, but less than 1:6), and >16.6% (greater than 1:6). These were labeled as cross grain 1, 2, and 3, respectively. Cross grain values less than 10% were classified as clear wood if no other defects were visible. In addition, regions of diving grain around knots, i.e., grain fiber direction normal to the wood surface, were also labeled. These "near knot" regions are not pallet part defects, per se, but were expected to give different TOF readings and therefore needed to be distinguished as a different class of wood. On the deckboard samples that we examined then, six classes of wood were identified: clear wood, cross grain 1, cross grain 2, cross grain 3, knots, and near_knots.

3.5 TOF value normalization

Because TOF values will differ for individual boards, boards of different thickness, different moisture contents, and different species, it was not possible to use absolute TOF values to categorize board regions. Rather, it became necessary to normalize TOF values so that data from different boards could be combined and so that data taken at different points in time could be treated identically. Typically, this is done by normalizing raw data values using the value of the clear wood region of an image⁷. An underlying assumption for this technique is that the relative location of important features' data values in an image histogram is invariant over time, between samples, and between species. Therefore, for example, image values for knot pixels will appear in the same location relative to the clear wood peak on a histogram regardless of what sample or species is being examined.

In most applications dealing with wood, scanned images will contain a large proportion of clear wood pixels. This is not the case, however, for pallet parts, where defect regions predominate an image. Therefore, it becomes much more difficult to visually or analytically estimate the average clear wood value for an image histogram. This effect was exacerbated in our study data because we only sampled approximately 1/2 of each board's length, and intentionally chose scan grid regions that included "interesting," i.e., defected areas.

Using the limited sets of TOF values for each board we were able to find an algorithmic procedure that agreed very well with clear wood TOF values obtained by the defect classification procedure described above. Basically, this procedure finds the average of the right-most sharp peak(s) of a histogram (Figure 2). It does this by finding the right-most "significant" trough of the histogram's derivative (h) and by finding the right-most "significant" peak of the histogram's derivative (a). These two values are averaged to obtain the normalizing values for that board's TOF values. Subsequent analyses used these normalized TOF values. More details on this normalizing technique and its accuracy are not included here.

4. RESULTS

Paired T-tests were performed on the repeated TOF measurements for QrD2 and QrD3 for both the 0.5 MHz and 1.25 MHz transducers. The tests on QrD2 showed no significant difference between the two sets of measurements for both transducers. This would indicate that the air-coupled rolling transducers can produce measurements that are repeatable. T-tests for the repeated measurements on QrD3, however, were highly significant for both transducers, indicating a significant difference between measurements. Further examination of the QrD3 data indicated that the T-test results are very dependent on the normalizing value used. In fact, by increasing the normalizing value from 6.7 to 6.9 microseconds for the repeated set of QrD3 values, it was possible to produce a non-significant test.

TOF images and gray-scale photos of the scan grids for the four samples appear in Figure 3. The TOF data depicted here were collected using the 84 KHz transducers, and the data were then normalized as described above. Darker regions on the TOF images indicate shorter times, typically associated with knot regions. From visual inspection, there appears to be some correlation between knot region and TOF values. Less visually striking, but noticeable, is the relationship between extreme cross grain regions and lower TOF values (darker pixels). A one-way ANOVA was performed for each transducer using the pooled data from all four deckboards. Significant ANOVA F-tests would indicate whether there were significant differences between class means for the six different regions noted above. The “knot” class had the fewest number of sample points (26). To generate a balanced ANOVA, 26 sample points were randomly selected from the other five classes. F-Test results for the 84 KHz, 0.5 MHz, and 1.25 MHz transducers were 21.24, 6.87, and 5.77, respectively. Each of these F values is highly significant ($p < 0.001$), indicating that differences exist between the mean TOF values for the different classes.

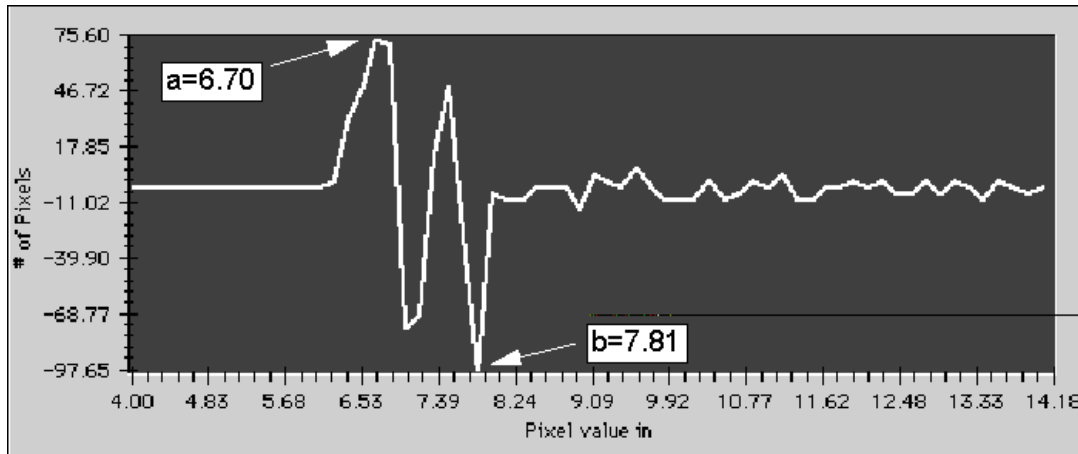


Figure 2. Derivative of the histogram for QrD2 (84 KHz) illustrates the selection of the trough and peak values and a , used for estimating a normalizing clear wood value.

F-test results for the 84 KHz transducer are much more statistically significant than results for the other 2 transducers. We performed post-hoc, pair-wise T-tests to determine which class means were significantly different for the 84 KHz transducer. The probability values associated with those tests appear in Table 2. Knot and Near_Knot regions have significantly different normalized TOF values than the other regions. Clear Wood, CG1, and CG2 regions are not significantly different from each other. CG3 is significantly different from CG2, but not from CG1. When we use a different random sample of 26 data points, we obtain a similar F statistic for the 84 KHz transducer (22.1). However, pair-wise T-test probability values differ somewhat (Table 3). In particular, Knots and CG3 are significantly different from all other regions, and Near_Knot areas are different from all except CG1 and CG2. Clear Wood areas remain indistinguishable from CG1 and CG2 in the second sample's tests.

Due to the variability of results using different random samples, we also examined results from an unbalanced ANOVA. In this case, all 1108 data points were used but the F-test value (60.38) is inflated because of the large number of samples from Clear Wood data points having a lower variance. ANOVA F-tests are sensitive to unequal variances among

treatments. However, because T-tests are much more robust with respect to uneven sample sizes and unequal variances, pair-wise probability values for the unbalanced design should still provide a good picture of where the true differences between class means lie (Table 4). Unbalanced design results indicate that: (1) Knots and Near_Knot points are very different from each other and from other classes, (2) CG3 points are fairly distinguishable from Clear Wood, CG1, CG2 points, and (3) Clear Wood, CG1, and CG2 are not distinguishable from each other based on single-point TOF values only.

5. CONCLUSIONS AND DISCUSSION

Repeatability tests on QrD2 and QrD3 deckboards are contradictory at this point. As noted above, however, the normalizing values used for each board can have a large impact on the significance of the tests. By using data from full board scans we hope to be able to estimate more reliable normalizing values. Subsequent repeatability tests should then be more conclusive than these preliminary ones. However, as noted below, the variability for the two transducers used in these repeatability tests tends to be higher than for the 84 KHz transducers, so repeatability may not, in fact, be a problem when using the latter. Less certain X-Y positioning with the portable roll-bed used with the 84 KHz transducers made measurement repeatability tests difficult to perform and to rely on.

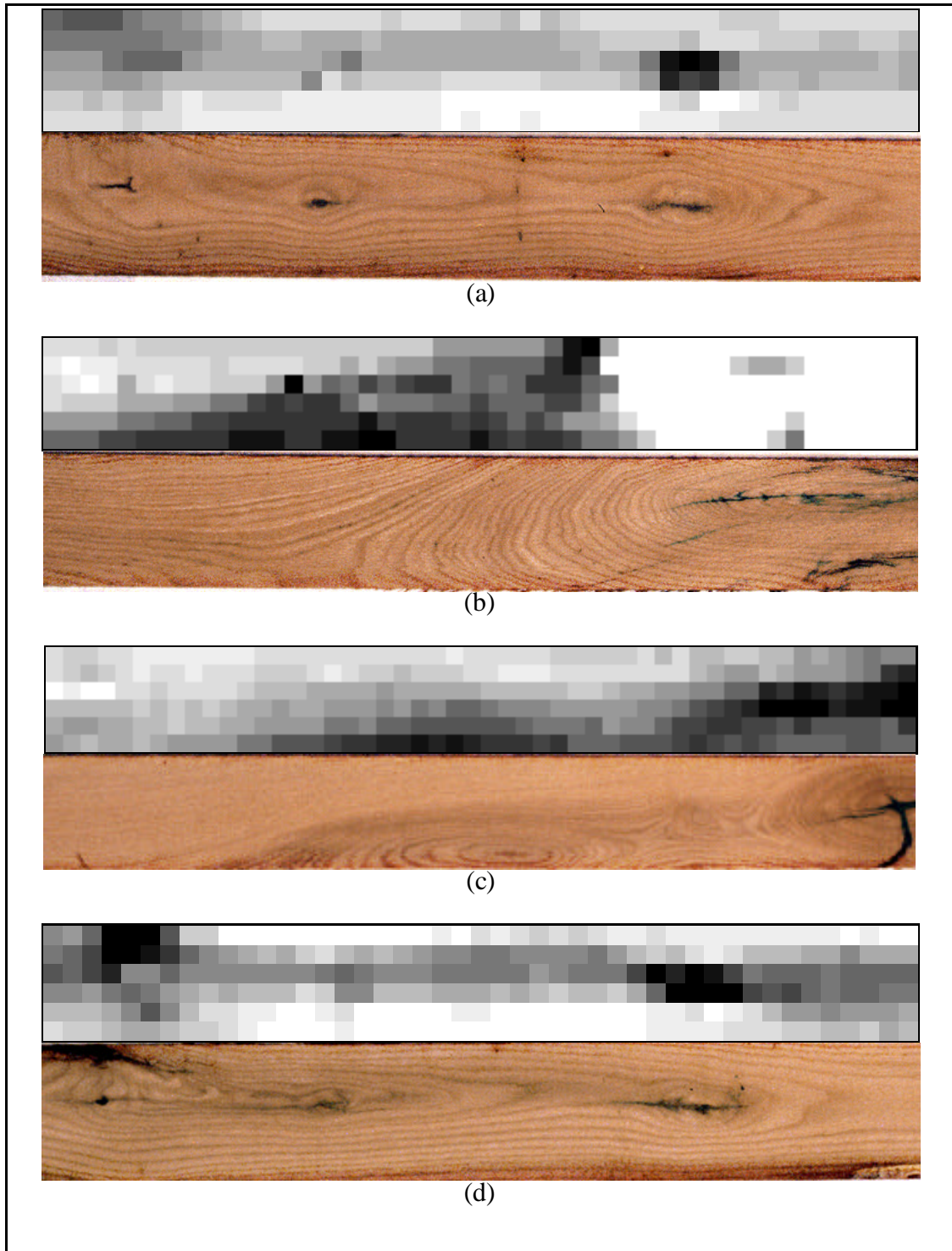


Figure 3. TOF images for the 84 KHz transducers and gray-scale photos of scan grids for deckboards: (a) QrD1, (b) QrD2, (c) QrD3, and (d) QrD5.

Table 2. One selection of 26 random samples produces these pair-wise T-test probability values for class mean difference TOF values (84 KHz transducer).

	Near_Knot	Knot	CG1	CG2	CG3	Clear Wood
Knot	0.016	1.000				
CG1	0.004	0.000	1.000			
CG2	0.030	0.000	0.993	1.000		
CG3	0.000	0.000	0.191	0.047	1.000	
Clear Wood	0.002	0.000	1.000	0.972	0.289	1.000

Table 3. A second selection of 26 random samples produces different pair-wise T-test probability values for class mean difference TOF values (84 KHz transducer).

	Near_Knot	Knot	CG1	CG2	CG3	Clear Wood
Knot	0.000	1.000				
CG1	0.200	0.000	1.000			
CG2	0.342	0.000	0.999	1.000		
CG3	0.000	0.000	0.011	0.004	1.000	
Clear Wood	0.048	0.000	0.992	0.954	0.063	1.000

The 84 KHz transducers seem to discriminate between board features better than the higher frequency transducers. This result is consistent with the observations of other researchers that 100-300 KHz ultrasonic frequencies are preferred for wood inspection. In addition to the 84 KHz frequency advantage, the use of larger diameter transducers also has some intuitive appeal. Because larger diameter piezo-electric elements average wood characteristics over a larger area than smaller transducer elements, they produce TOF values with a smaller variance. This reduced variance might give 84 KHz transducers better repeatability than the higher frequency transducers, with their higher variance. This results in less variable pixel TOF values within a particular class relative to between-class variation, hence F-test statistics are larger in magnitude.

Normalized TOF values allow us to easily distinguish Knot, Near_Knot, and CG3 defects from other wood features. Less severe levels of cross grain (CG1 and CG2), on the other hand, are not so easily discriminated. This is due in part to the fact that cross grain is difficult to measure using either visual inspection or slope-of-grain measuring equipment. Despite the limitations of TOF measurements to discriminate cross grain classes for individual pixels, we do not expect ultimately that individual, pixel TOF values will be exclusively used to classify image pixels. We feel that, in the future, it will be necessary to use some measure of spatially varying TOF values, i.e. texture, to actually label each pixel of an image.

A texture analysis approach will use pixel values surrounding each pixel of an image to label that pixel. It is possible that there will be information in a neighborhood of pixels that can improve on the single-pixel, TOF relationships identified in this study.

Table 4. The complete, unbalanced ANOVA (1108 data points) produces these pair-wise T-test probability values for class mean difference TOF values (84 KHz transducer).

	Near_Knot	Knot	CG1	CG2	CG3	Clear Wood
Knot	0.000	1.000				
CG1	0.000	0.000	1.000			
CG2	0.000	0.000	0.995	1.000		
CG3	0.000	0.000	0.075	0.027	1.000	
Clear Wood	0.000	0.000	1.000	0.983	0.087	1.000

6. REFERENCES

1. V. S. Reddy, R. J. Bush, and P. A. Araman, "Pallets: The new hardwood resource," *Center for Forest Products Marketing, Virginia Tech Report to Members*, November 1996.
2. D. L. Schmoldt, J. A. McCleod III, and P. A. Araman, "Economics of grading and sorting pallet parts," *Forest Products Journal* Vol. 43, No. 11/12, pp. 19-23, 1993.
3. K. A. McDonald, "Lumber defect detection by ultrasonics," *U.S. Department of Agriculture, Forest Service Res. Pap. FPL-311*, Forest Products Lab, Madison WI, 1980.
4. K. A. McDonald, R. G. Cox, and E. H. Bulgrin, "Locating lumber defects by ultrasonics," *U.S. Department of Agriculture, Forest Service Research Paper FPL-120*, Forest Products Lab, Madison WI, 1969.
5. M. Patton-Mallory and R. C. DeGroot, "Detecting brown-rot decay in southern yellow pine by acousto-ultrasonics," *Proceedings of the 7th International Nondestructive Testing of Wood Symposium*, pp. 29-44, Conference and Institutes, Washington State University, 1990.
6. W. W. Wilcox, "Detection of early stages of wood decay with ultrasonic pulse velocity," *Forest Products Journal*, Vol. 38, No. 5, pp. 68-73, 1988.
7. J. L. Sandoz, "Grading of construction timber by ultrasound," *Wood Science and Technology* Vol. 23, pp. 95-108, 1989.
8. U. B. Halabe, H. V. S. GangaRao, and V. R. Hota, "Nondestructive evaluation of wood using ultrasonic time and frequency domain analysis," *Review of Progress in Quantitative Nondestructive Evaluation*, eds. D. O. Thompson and D. E. Chimenti, Vol. 13, pp. 2155-2160, Plenum Press, New York, 1994.

9. U. B. Halabe, H. V. S. GangaRao, and V. R. Hota; "Nondestructive evaluation of wood using ultrasonic frequency domain analysis," *Review of Progress in Quantitative Nondestructive Evaluation* eds. D. O. Thompson and D. E. Chimenti, Vol. 14, pp. 1653-1660, Plenum Press, New York, 1995.
10. U. B. Halabe, H. V. S. GangaRao, S. H. Petro, and V. R. Hota; "Assessment of defects and mechanical properties of wood members using ultrasonic frequency analysis," *Materials Evaluation*, Vol. 54, No. 2, pp. 314-322, 1996.
11. U. B. Halabe and C. E. Solomon; "Nondestructive evaluation of wood using ultrasonic dry-coupled transducers," *Review of Progress in Quantitative Nondestructive Evaluation* eds. D. O. Thompson and D. E. Chimenti, Vol. 12, pp. 2251-2256, Plenum Press, New York, 1993.
12. R. L. Lemaster and D. A. Dornfeld, "Preliminary investigation of the feasibility of using acousto-ulasonics to measure defects in lumber," *Journal of Acoustic Emission* Vol. 6, No. 3, pp. 157-165, 1987.
13. J. J. Fuller, R. J. Ross, and J. R. Damm, "Honeycomb and surface check detection using ultrasonic nondestructive evaluation," *U.S. Department of Agriculture, Forest Service Research Note FPL-RN-0261*, Forest Products Laboratory, Madison WI, 1994.
14. C. M. Fortunko, M. C. Renken, and A. Murray, "Examination of objects made of wood using air-coupled ultrasound," *Proceedings of the 1990 Ultrasonics Symposium* ed. B. R. McAvoy, pp. 1099-1103, 1990.
15. D. L. Schmoldt, J. C. D. Jr., M. Morrone, and C. M. Jennings, "Application of ultrasound nondestructive evaluation to grading pallet parts," *9th International Symposium on Nondestructive Testing of Wood* eds. R. Pellerin and K. A. McDonald, pp. 183-190, Conferences and Institutes, Washington State University, 1994.
16. D. L. Schmoldt, M. Morrone, and J. C. D. Jr.; "Ultrasonic inspection of wooden pallet parts for grading and sorting," *Review of Progress in Quantitative Nondestructive Evaluation* eds. D. O. Thompson and D. E. Chimenti, Vol. 12, pp. 2161-2166, Plenum Press, New York, 1994.
17. D. L. Schmoldt, P. Li, and A. L. Abbott, "Machine vision using artificial neural networks and 3D pixel neighborhoods," *Computers and Electronics in Agriculture* In press, 1996.



PROCEEDINGS
SPIE—The International Society for Optical Engineering

Nondestructive Evaluation of Materials and Composites

Steve Doctor
Carol A. Lebowitz
George Y. Baaklini
Chairs/Editors

3-5 December 1996
Scottsdale, Arizona

Sponsored by
SPIE—The International Society for Optical Engineering

Cosponsored by
Federal Highway Administration
Nondestructive Testing Information Analysis Center
Air Force Wright Laboratory
Pressure Vessel Research Council
The Materials Properties Council, Inc.

Cooperating Organizations
U.S. Department of Energy
DARPA
National Institute of Standards and Technology
Lawrence Livermore National Laboratory
Society for Experimental Mechanics
American Society of Mechanical Engineers
Federal Aviation Administration
American Society for Testing and Materials
CalTrans
Electric Power Research Institute
Battelle Pacific Northwest National Laboratory

Published by
SPIE—The International Society for Optical Engineering



Volume 2944

SPIE is an international technical society dedicated to advancing engineering and scientific applications of optical, photonic, imaging, electronic, and optoelectronic technologies.